Korean J. Electron Microscopy Special Issue 1, 1 ~ 7(2006)

HVEM Application to Electron Crystallography: Structure Refinement of $SmZn_{0.67}Sb_2$

Jin-Gyu Kim, Young-Min Kim, Ji-Soo Kim and Youn-Joong Kim*
Electron Microscopy Team, Korea Basic Science Institute, 52 Yeoeun-Dong,
Yusung-Gu, Daejeon, 305-333, Korea
(Received April 6, 2005; Accepted March 24, 2006)

ABSTRACT

The three-dimensional structure of an inorganic crystal, $SmZn_{0.67}Sb_2$ (space group $P4/nmm$, a=4.30(3)Å and c=10.27(1)Å), was refined by electron crystallography utilizing high voltage electron microscopy (HVEM). Effects of instrumental resolution, image quality, beam damage and specimen tilting on the structure refinement have been evaluated. The instrumental resolution and image quality were the most important factors on the final results in the structure refinement, while the beam damage and specimen tilting effects could be experimentally minimized or controlled. The average phase errors (ϕ_{res}) for the [001], [100] and [110] HVEM images of $SmZn_{0.67}Sb_2$ were 10.1°, 9.6° and 6.8°, respectively. The atomic coordinates of $SmZn_{0.67}Sb_2$ were consistent within 0.0013Å ~ 0.0088Å, compared to the X-ray crystallography data for the same sample.

Key words : Electron crystallography, High voltage electron microscopy (HVEM), Inorganic crystal, Structure refinement

INTRODUCTION

A goal of crystal structure studies by electron crystallography is to determine the atomic positions in the unit cell to the level of X-ray crystallography. Compared to X-ray diffraction, electron diffraction has not been widely used for structure determination even though it should be an important technique for solving crystal structures. One of the essential problems responsible for this slow development of electron crystallography is the dynamical nature of electron scattering (Zou, 1995; Dorset, 1995; Dorset et al., 1997). On the other hand, electron crystallography has several advantages, which include possibility to use very small amount of samples, determination of very local structures and direct solution of phase problem that is difficult in X-ray crystallography.

Generally, there are two methods for the structure determination by electron crystallography, that is, HRTEM image analysis and quantitative electron diffraction (QED) analysis (Gilmore, 2003). In case of the former, crystallographic image processing (CIP) and exit wave reconstruction method have been developed (Hovmöller, 1992; Zandbergen et al., 1999). In case of the latter, Pattern analysis, direct methods and maximum entropy methods have been developed (Altomare et al., 1999; Gilmore, 1999; Bougerol-Chaillout, 2001).

In this paper, we carried out structure refinement by the CIP method utilizing high resolution HVEM images. Effects of instrumental resolution, image quality, beam demage and specimen tilting on the structure refinement have been evaluated.

EXPERIMENTAL METHODS

The initial structure refinement of $SmZn_{0.67}Sb_2$ was reported in our previous paper (Kim et al., 2004). HRTEM images were obtained to compare the instru-

* Correspondence should be addressed to Dr. Youn-Joong Kim, Electron Microscopy Team, Korea Basic Science Institute, 52 Yeoeun-Dong, Yusung-Gu, Daejeon, 305-333, Korea. Ph.: (042) 865-3596, FAX: (042) 865-3939, E-mail: y-jkim@kbsi.re.kr

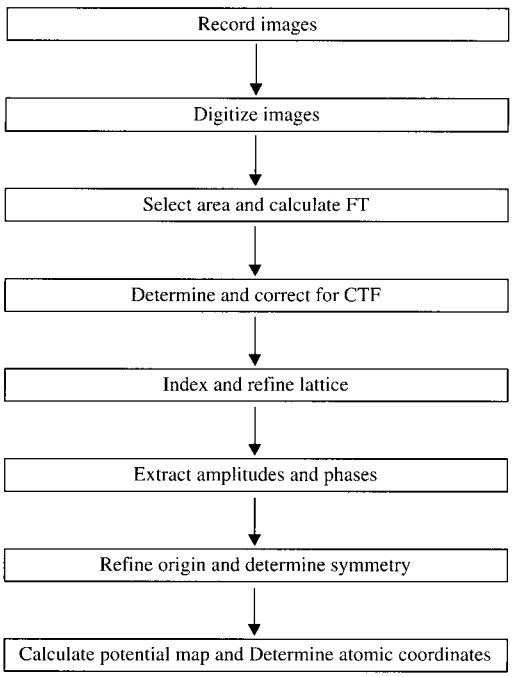

Fig. 1. General procedures for structure refinement by HRTEM images.

mental resolution effect between JEM-ARM 1300S (point resolution 1.17Å at 1,250 kV, LaB_6 gun, HVEM) and JEM-2100F (point resolution 1.9Å at 200 kV, field emission gun, FE-TEM). General procedures for electron crystallography shown in Fig. 1 were employed, but all instrumental conditions such as specimen thickness, focus conditions and tilting were more strictly controlled (Zou, 1995; Kim et al., 2004). Magnification calibration of HVEM images was performed with a standard sample using the Digital Micrograph program (Gatan Inc.) and the CIP procedure was performed using the CRISP program (Hovmöller, 1992).

RESULTS AND DISCUSSION

1. Instrumental resolution effect

In case of the HRTEM image analysis, image resolution is the most important parameter because the phase and amplitude information of all atoms must be extracted directly from the images. To evaluate this resolution effect the [100] HRTEM images of $SmZn_{0.67}Sb_2$ were obtained using the HVEM and FE-TEM. Fig. 2 clearly

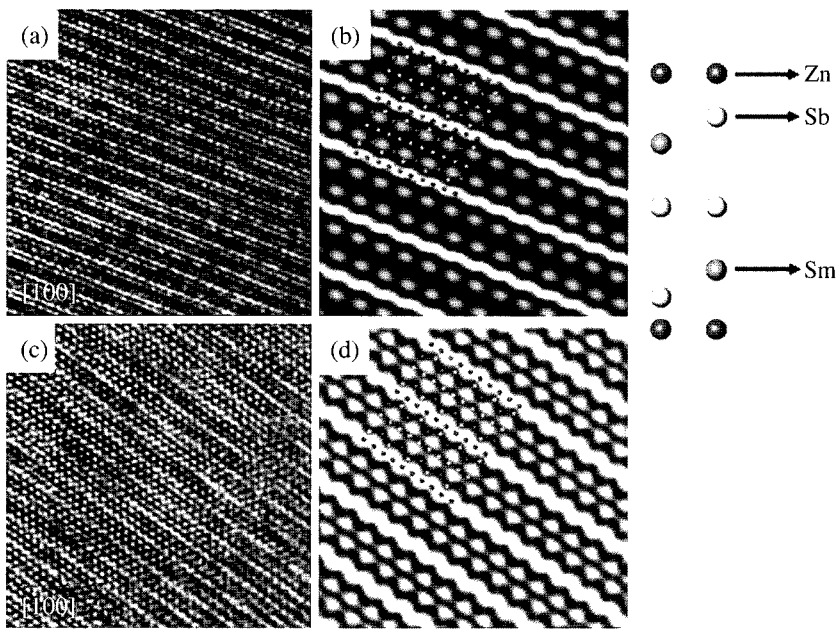

Fig. 2. The [100] HRTEM images obtained by two different instruments: (a) and (c) are original images by FE-TEM and HVEM; (b) and (d) are their processed images.

shows the advantage of HVEM over FE-TEM by overlaying the atomic structure model on the processed images. It was expected that the phase errors for the FE-TEM images should be larger than those of the HVEM images because the atomic site was not resolved within the layer plane. Actually, as a results of the CIP processing, the phase errors (ϕ_{res}) by FE-TEM and HVEM were 19.0° and 9.6°, respectively. In case of HVEM application, it was possible to determine some of the atomic coordinates with nearly 1Å resolution in thin inorganic crystals. In addition, the HVEM images contain more kinematical information than those of the FE-TEM images because the dynamical scattering effect depends on the penetration power.

2. Image quality effect by CTF determination

For a weak phase object from the thinnest part of the crystal, the Fourier transform of the image I(u) is related to the Fourier transform of the projected potential $\phi(u)$ by

$$I(u)=D(u)\sin(\chi)\Phi(u)$$

where $D(u)\sin(\chi)$ is the contrast transfer function (CTF), D(u) is the damping function of the CTF and

$$\chi(u)=\left(\pi\varepsilon\lambda u^2+\frac{(\pi C_s\lambda^3u^4)}{2}\right)$$

where ε is the defocus value, C_s is the spherical aberration constant and λ is the wavelength. Therefore there are two ways to determine the CTF. The one is to determine the defocus value and the other is to determine the position u of the CTF crossover. The defocus value as variation of the CTF crossover position was shown in Fig. 3. It is presented obviously that the projected potential maps by the CIP processing depend on determination of the defocus values. The phase errors of Fig. 3(c) and (d) are smaller than that of Fig. 3(a), which is nearly in the Scherzer focus, but the structure is not solvable due to its poor RA (5) values. If the clear dark rings from the amorphous area are included in the Fourier transformed image, the defocus value and the crossover position u of the CTF could be determined accurately. Unfortunately, the defocus value could not be determined accurately in this HVEM image due to lack of the amorphous area.

In order to estimate the defocus value, the Fourier filtered image from the [110] original image was compared with the simulation images by the JEMS program (Fig. 4). The preliminary step for determination of the defocus value by image simulation was to process the original image (Fig. 4(a)-(d)). Image simulation was performed by controlling defocus values and thicknesses, which resulted in the estimated defocus value between −35 nm and −40 nm in Fig. 4(e). If only the CTF is determined accurately, the projected potential

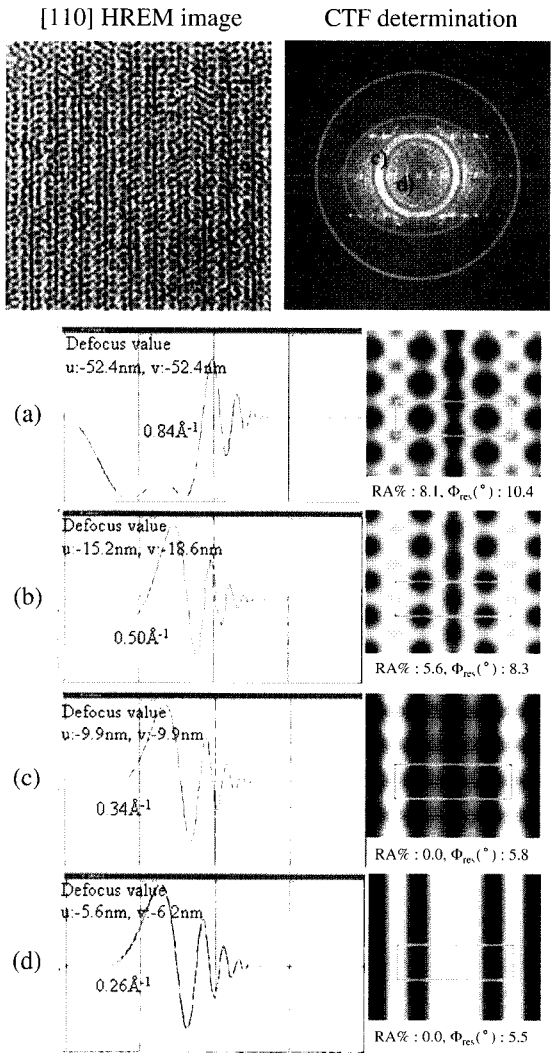

Fig. 3. CIP processing results of the [110] HVEM image as the CTF determination: each defocus values is −52.4 nm, −15.2 nm, −9.9 nm, −5.6 nm for (a), (b), (c) and (d), respectively. It was assumed that (b) included astigmatism determination.

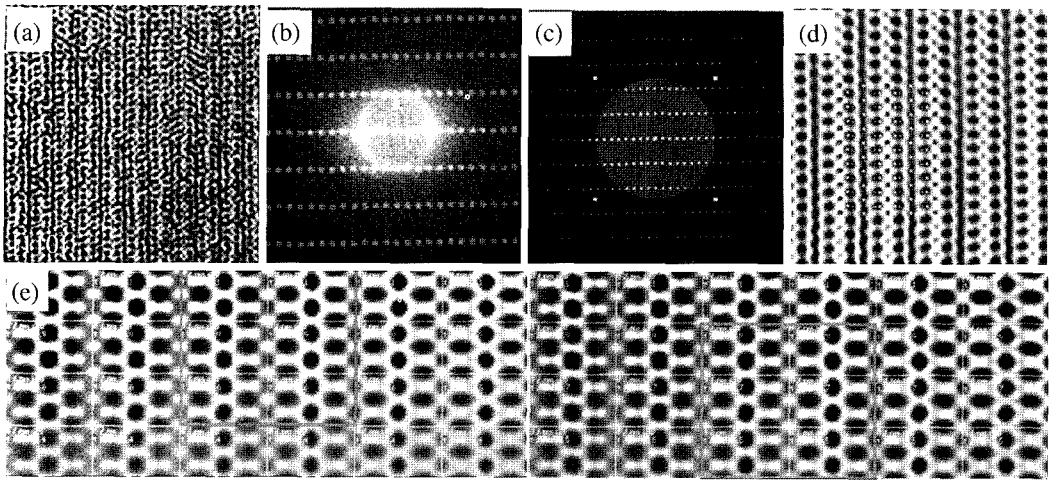

Fig. 4. Determination of the thickness and defocus values by image simulation: (a) [110] original image; (b) pattern masking on the FT image of (a); (c) band pass masking; (d) final processed image; (e) simulated images by JEMS.

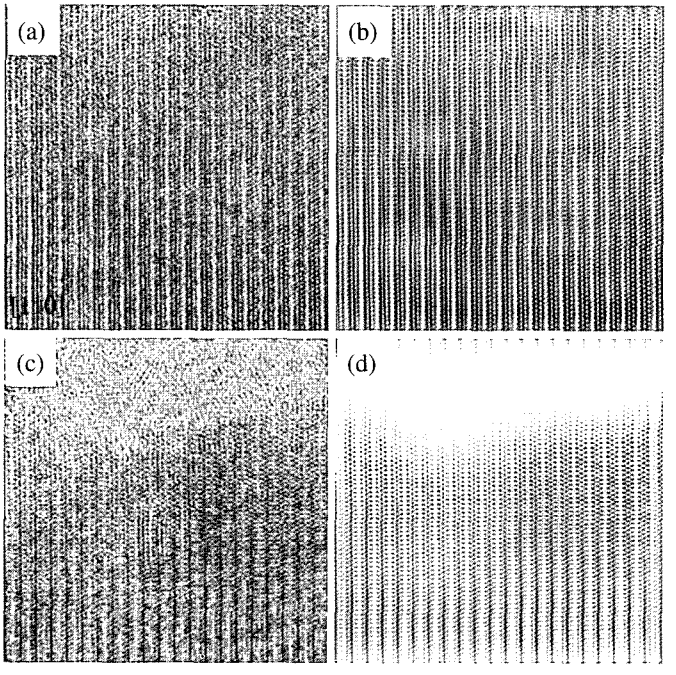

Fig. 5. Irradiation damage in $SmZn_{0.67}Sb_2$, during the through-focus imaging: (a) initial image; (b) processed image of (a); (c) image after beam irradiation; (d) processed image of (c).

map could be retrieved from HRTEM images under the non-optimum conditions (Zou, 1996). The phase error of the [110] HVEM image was determined with the defocus value and the crossover position estimated from the image simulation, which is shown in Table 2.

3. Beam irradiation effect

Since specimens are irradiated by intense electrons in the HVEM experiment, beam damage is often induced and the materials transformed from crystalline to amorphous structure. The $SmZn_{0.67}Sb_2$ crystal structure also undergoes beam-induced transformation during through-focus imaging and specimen tilting (Figs. 5, 6). For the structure determination only, however, the beam damage effect on structure refinement could be avoided by taking the undamaged area. On the other hand, it is even possible to use amorphous structure of the damaged area to evaluate the optimum defocus value.

4. Specimen tilting effect

For three-dimensional structure analysis, the specimen tilting works from the [110] zone axis to the [100] zone axis were carried out (Fig. 6). The direct tilting angle between these two zone axes was calculated from the experimental data by the method described in the previous paper (Kim et al., 2004). The thickness variation was estimated using the trigonometric function. Thickness increase due to specimen tilting degraded the image quality and increased the phase errors (Table 1). To reduce the tilting effect, the tilting direction of the goniometer should be toward the zero-tilt position. This tilting effect may be reduced by energy-filtering, especially plasmon-loss HRTEM imaging, which is currently investigated.

Table 1. The thickness variation and phase errors due to specimen tilting

	Original thickness (by JEMS)	Tilting angle (°)		Thickness variation (nm)	ϕ_{res} (°)
[110]	3.56~7.81 nm	6.31	−6.09	3.6~7.90	6.8
[100]		30.03	34.64	4.99~10.96	9.6

5. Comparison of the initial and final structure refinements

In comparison with our previous results (Kim et al., 2004), several effects, such as instrumental resolution, image quality by the CTF correction, beam irradiation, specimen tilting on the $SmZn_{0.67}Sb_2$ structure refinement have been evaluated. The final refinement results for the three major zone axes, [001], [100], and [110], were displayed in Fig. 7. Three original images (Fig. 7

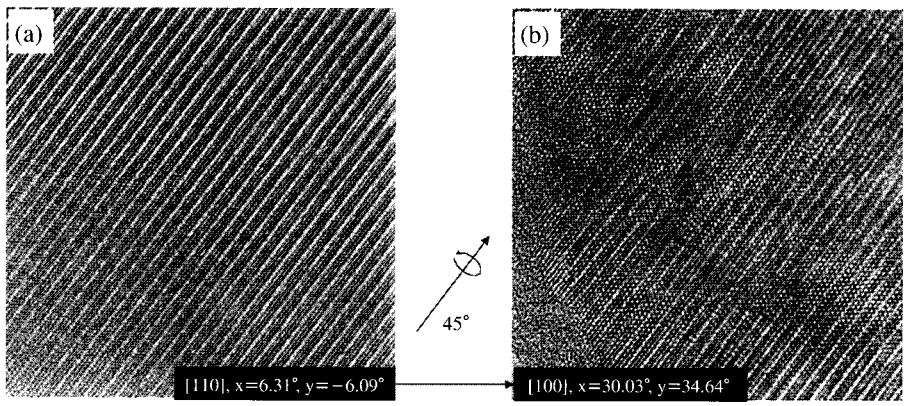

Fig. 6. The thickness variation by specimen tilting from the [110] to [100] zone axes.

Table 2. Comparison of the crystallographic data and reliability results

Zone axis	X-ray	1st refinement			2nd refinement		
		Cell parameters (Å)	RA (%)	ϕ_{res} (°)	Cell parameters (Å)	RA (%)	ϕ_{res} (°)
[001]	a=4.2976Å, c=10.287Å	a=4.29, b=4.29	46.0	17.0	a=4.33, b=4.33	24.4	10.1
[100]		a=10.39, b=4.21	34.8	8.3	a=10.26, b=4.27	2.4	9.6
[110]		a=10.32, b=3.03	37.8	21.9	a=10.28, b=3.19	8.4	6.8

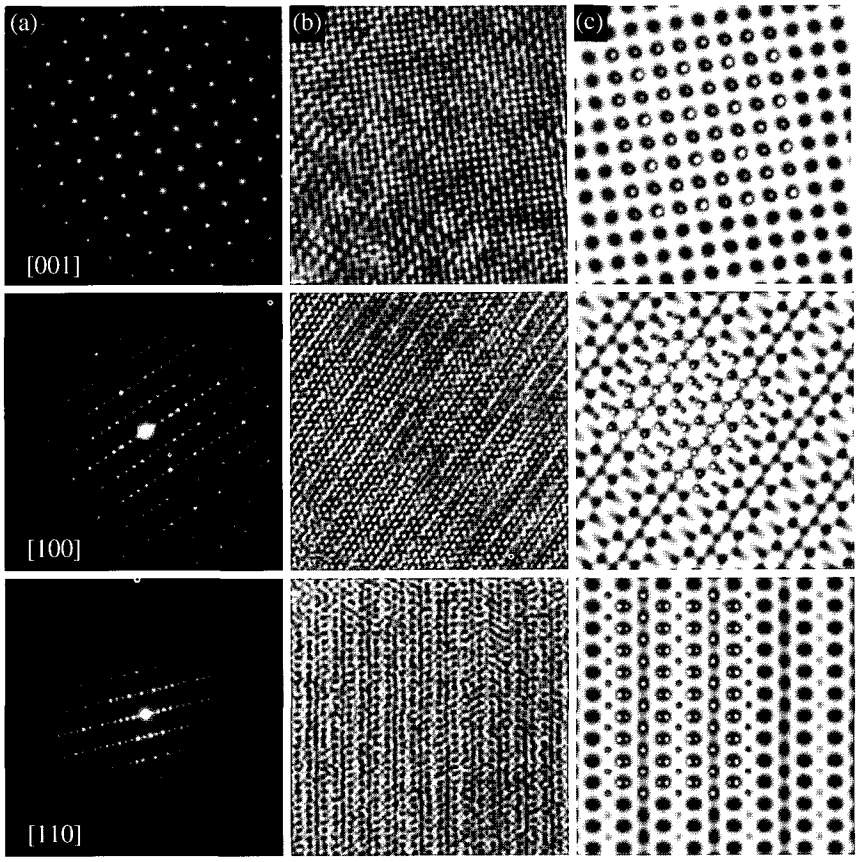

Fig. 7. The final refinement of the three major zone axes [001], [100], and [110]: a) ED patterns of the corresponding zone axes; b) original averaged images; c) the final projected potential maps.

Table 3. Comparison of the atomic coordinates between the two refinements

Atoms	1st refinement						2nd refinement					
	Coordinates			Dev. compared to X-ray			Coordinates			Dev. compared to X-ray		
	x	y	z	Δx	Δy	Δz	x	y	z	Δx	Δy	Δz
Sm	0.250	0.250	0.272	0.0	0.0	−0.0097	0.250	0.250	0.272	0.0	0.0	−0.0088
Sb(1)	0.250	0.250	0.827	0.0	0.0	0.0107	0.250	0.250	0.839	0.0	0.0	−0.0013
Sb(2)	0.750	0.251	0.503	0.0	0.00	−0.003	0.750	0.250	0.500	0.0	0.0	0.0
Zn	0.750	0.252	0.005	0.0	0.002	−0.005	0.750	0.750	0.000	0.0	0.0	0.0

(b)) obviously indicate their higher quality than those in the previous reports. Even if the visible effect is not distinct in the final projected potential map itself, it is certain that the higher quality images bring out significant improvement of the phase errors.

As listed in Table 2, the cell parameters of $SmZn_{0.67}Sb_2$ are a=4.25(4)Å and c=10.35(4)Å in the first refinement, while a=4.30(3)Å and c=10.27(1)Å in the second refinement. Also, phase errors are significantly reduced except for the [100] HVEM image. It is believed that this phase error is related to the thickness increase due to the specimen tilting from [110] to [100] in

the second refinement, compared to the specimen tilting tilting from [100] to [110] in the first refinement.

The atomic coordinates from these two refinements are shown in Table 3. As might be expected, the atomic coordinates at the general positions (especailly Sb atom) as well as the special positions were determined more accurately in the second refinement. They were also consistent with the X-ray crystallographic data within 0.0013~0.0088Å. For more accurate retrieval of amplitudes and phases, however, the quantitative electron diffraction data is desired to be combined with the image data.

CONCLUSIONS

The crystal structure of an inorganic crystal, $SmZn_{0.67}Sb_2$, was solved by electron crystallography mainly utilizing HVEM. Several experimental effects on the final results were evaluated and the following conclusions are established in this experiment:

1) High-resolution, high-quality images significantly improved the final results in the CIP procedure for the structure refinement.

2) Although the beam irradiation and specimen tilting increase the phase errors, their effects on the structure refinement could be experimentally minimized or controlled.

3) The average phase errors (ϕ_{res}) for the [001], [100] and [110] HVEM images were 10.1°, 9.6° and 6.8°, respectively.

4) The atomic coordinates of $SmZn_{0.67}Sb_2$ were consistent within 0.0013~0.0088Å, compared to the X-ray crystallography data for the same sample.

REFERENCES

Altomare A, Burla MC, Camalli M, Cascarano G, Giacovazzo C, Guagliardi A, Moliterni AGG, Polidori G, Spagna R: J Applied Crystallography 32 : 115, 1999.

Bougerol-Chaillout C: Micron 32 : 473, 2001.

Dorset DL: Structural Electron Crystallography. Plenum Press, New york and London, pp. 135. 1995.

Dorset DL, Hovmöller S, Zou XD (eds): Electron Crystallography. Kluwer Academic Publishers, Dordrecht/Boston/London, pp. 439, 1997.

Gilmore CJ: Microscopy Research and Technique 46 : 117, 1999.

Gilmore CJ: Crystallography Reviews 9 : 17, 2003.

Hovmöller S: Ultramicroscopy 41 : 121, 1992.

Kim JG, Kang SK, Kim WC, Kim YJ: Korean J Electron Microscopy 34 : 255, 2004.

Zandbergen HW, Bokel R, Connolly E, Jansen J: Micron 30 : 395, 1999.

Zou XD: Electron Crystallography of Inorganic Structures. Stockholm, pp. 1, 1995.

Zou XD, Sundberg M, Larine M, Hovmöller S: Ultramicroscopy 62 : 103, 1996.